ORGANOMETALLICS
Article
Cite This: Organometallics 2018, 37, 2991−3000
pubs.acs.org/Organometallics

Syntheses, Structures, and Thermal Properties of Gyroscope-like Complexes Consisting of $PtCl_2$ Rotators Encased in Macrocyclic Dibridgehead Diphosphines $P((CH_2)_n)_3P$ with Extended Methylene Chains (n = 20/22/30) and Isomers Thereof

Sugam Kharel,[†] Hemant Joshi,[†] Nattamai Bhuvanesh, and John A. Gladysz*

Department of Chemistry, Texas A&M University, P.O. Box 30012, College Station, Texas 77842-3012, United States

Supporting Information

ABSTRACT: Reactions of $P((CH_2)_mCH{=}CH_2)_3$ (2.0 equiv; m = 9 (**f**), 10 (**g**), 14 (**k**)) and $PtCl_2$ in toluene give *trans*-$PtCl_2(P((CH_2)_mCH{=}CH_2)_3)_2$ (*trans*-**1f,g,k**; 63−49%). Reactions of *trans*-**1f,g** with Grubbs first generation catalyst (CH_2Cl_2/reflux) followed by hydrogenations (cat. PtO_2) afford chromatographically separable gyroscope-like *trans*-$PtCl_2(P((CH_2)_n)_3P)$ (*trans*-**2f,g**, 3−19%; from *inter*ligand metathesis) and *trans*-$PtCl_2(P((CH_2)_{n-1}CH_2)(CH_2)_nP((CH_2)_{n-1}CH_2))$ (*trans*-**2′f,g**, 25−12%; from *inter*- and *intra*ligand metathesis), where $n = 2m + 2$. Under analogous conditions, *trans*-**1k** gives only *cis*-$PtCl_2(P((CH_2)_{30})_3P)$ (*cis*-**2k**, 39%), but when *o*-$C_6H_4Cl_2$ solutions are kept at 180 °C, *trans*-**2k** forms (quantitative by ^{31}P NMR; 72% isolated). In contrast, a similar sequence with the Hoveyda−Grubbs second generation catalyst gives only *trans*-**2k** (8%). The stability order *cis* > *trans* is established for **1g** and **2′f,g** in CH_2Cl_2 (61−56:39−44; months at RT), but the opposite is found for **1g** and **2′f** in toluene (9−7:91−93) or **2′f** in *o*-$C_6H_4Cl_2$ (7:93). Thus, it is proposed that the conversion of *trans*-**1k** to *cis*-**2k** involves a geometrical isomerization of the educt or an intermediate catalyzed by a species derived from Grubbs catalyst. The crystal structures of *trans*-**2g**·THF and *cis*-**2′f,g** are determined and analyzed in detail.

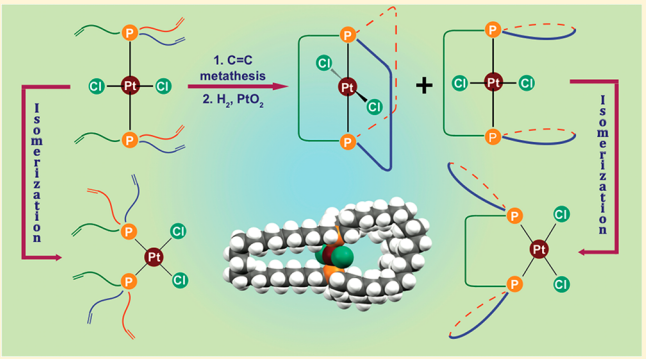

INTRODUCTION

The design and synthesis of sterically protected molecular rotors is under intense study in a number of laboratories.[1−13] In many cases, these are envisioned as components of various types of molecular devices.[14] In previous efforts, we have reported ring-closing alkene metatheses of platinum bis(phosphine) dichloride complexes of the formula *trans*-$PtCl_2(P((CH_2)_mCH{=}CH_2)_3)_2$ (*trans*-**1**)[15] with Grubbs first generation catalyst and subsequent hydrogenations.[16,17] When m is 6−8, gyroscope-like platinum complexes of the formula *trans*-$PtCl_2(P((CH_2)_n)_3P)$ (*trans*-**2**; n = 14 (**c**), 16 (**d**), 18 (**e**)) can be isolated, where n is the number of carbon atoms in the methylene chains ($n = 2m + 2$).[16,17] As shown in Scheme 1, these feature cage-like, triply *trans* spanning dibridgehead diphosphine ligands.

In some cases, the yields of *trans*-**2** are modest. However, trigonal bipyramidal $Fe(CO)_3$ adducts of the same dibridgehead diphosphines (as well as homologues with fewer methylene groups) can be similarly accessed in higher yields, as rationalized elsewhere.[18−20] Palladium analogues of *trans*-**2** have also been described.[16,17] With all MCl_2 adducts, rotation is fast on the NMR time scale, even at −100 °C.

In all of the above reactions, varying amounts of isomeric monoplatinum co-products, *trans*-$PtCl_2(P((CH_2)_{n-1}CH_2)(CH_2)_nP((CH_2)_{n-1}CH_2))$ (*trans*-**2′a−c**), have also been isolated.[17] Whereas *trans*-**2a−c** are derived from three-fold *inter*ligand alkene metathesis, *trans*-**2′a−c** are derived from combinations of *intra*ligand (two-fold) and *inter*ligand (single-fold) metathesis. The latter cyclization mode has also been seen with other metal fragments. However, except for a few octahedral systems with certain values of n,[21,22] it is always a minor pathway. Density functional theory (DFT) calculations (gas phase) suggest that *trans*-**2** is more stable than *trans*-**2′** for $n < 16$, but *trans*-**2′** is more stable for $n \geq 20$.[23,24]

We have sought to fully explore the topological space associated with the preceding compounds, as well as the free diphosphine ligands, and have systematically targeted various types of stereoisomers that may be isolable.[23,25] One of these, *trans*-**2″** in Scheme 1, is also derived from three-fold interligand alkene metathesis, but two of the methylene chains "cross", unlike

Received: May 22, 2018
Published: August 29, 2018

DOI: 10.1021/acs.organomet.8b00345
Organometallics 2018, 37, 2991−3000

Scheme 1. Three-Fold Ring-Closing Metatheses of *trans*-1c−e: Syntheses of Gyroscope-like Complexes *trans*-2c−e

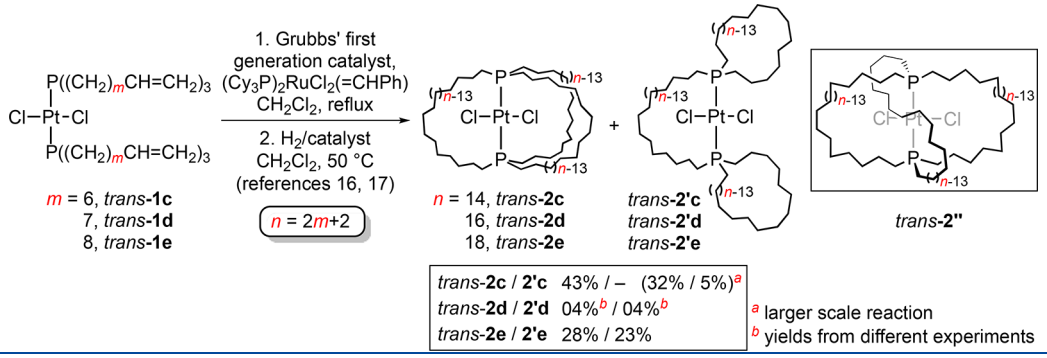

the disposition in *trans*-**2**. A *di*metallic adduct of a bridgehead diphosphine and a free dibridgehead diphosphine dioxide with crossed methylene chains have in fact been isolated.[25,26]

Another variable is the *cis*/*trans* sense at platinum. First consider the educts **1**. Only *trans*-**1b−e**, which lack permanent dipole moments, are obtained when the precursors are reacted in the nonpolar solvent benzene.[15] In contrast, *cis*-**1b−g**, which are shown in Scheme 2 and have dipole moments, dominate when

Scheme 2. Three-Fold Ring-Closing Metatheses of *cis*-1b−g: Syntheses of Parachute-like Complexes *cis*-2b−g

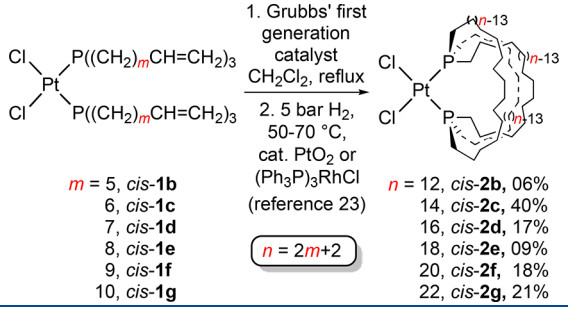

syntheses are carried out in the polar solvent water.[15,23] Related phenomena have been observed with other bis(phosphine) platinum dichloride complexes.[27] In any event, *cis*-**1b−g** undergo three-fold interligand alkene metathesis followed by hydrogenation to give *cis*-**2b−g** (Scheme 2).[23] For reasons detailed elsewhere, such complexes are often referred to as parachute-like[23]—a counterpart to the gyroscope-like attribute of *trans*-**2**. When kept in halobenzene solutions at 150−185 °C, *cis*-**2c,g** isomerize to *trans*-**2c,g**.[23] DFT calculations indicate the gas-phase stability trend *trans* > *cis* for **2a−g**.[23]

In this study, we sought to extend the syntheses of gyroscope-like complexes *trans*-**2** in Scheme 1 to higher values of *n*. Questions to be addressed included the following: (1) Might additional types of products, such as *trans*-**2″**, form? (2) How do *trans*-**2**/*trans*-**2′** selectivities vary? (3) Is the stability order *trans*-**2** > *cis*-**2** maintained? Additional motivation was provided by earlier observations that reactions of *trans*-**2c,e** and excesses of appropriate nucleophiles liberate the dibridgehead diphosphines **3c,e**, as shown in Scheme 3.[28−30] These can serve as "container molecules" for the selective transport of $PtCl_2$ and $PdCl_2$ away from $NiCl_2$.[30] It was thought that diphosphines with larger macrocycles might exhibit complementary selectivities, as well as other interesting chemistry.

RESULTS

Syntheses of the Title Compounds. The alkene containing phosphines $P((CH_2)_mCH{=}CH_2)_3$ were prepared

Scheme 3. Syntheses of Dibridgehead Diphosphines 3c,e

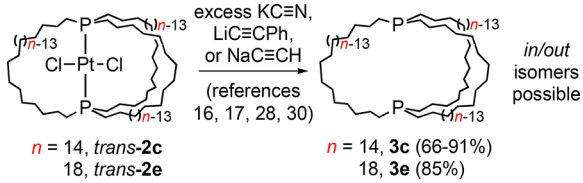

from PCl_3 and Grignard reagents $MgBr(CH_2)_mCH{=}CH_2)_3$ as described earlier ($m = 9$)[15,23] or by applying analogous protocols to Grignard reagents with longer methylene chains (m = 10, 14; Experimental Section). As shown in Scheme 4, $PtCl_2$ and the phosphines (2.0 equiv) were combined in the nonpolar solvent toluene. Workups gave the new platinum complexes *trans*-$PtCl_2(P((CH_2)_mCH{=}CH_2)_3)_2$ (*trans*-**1f,g,k**) as yellow oils or solids in 49−63% yields.

Complexes *trans*-**1f,g,k** and all other homogeneous new species below were characterized by IR and NMR (^1H, $^{13}C\{^1H\}$, $^{31}P\{^1H\}$) spectroscopy. Satisfactory microanalyses were also obtained. The $^1J_{PPt}$ values (2382−2375 Hz) were characteristic of *trans* stereoisomers[31] and much lower than those of *cis*-**1a−g** (3511−3518 Hz).[23] Other spectroscopic properties were similar to those of the lower homologues in Scheme 1.

As shown in Scheme 4, dilute CH_2Cl_2 solutions of the two complexes with shorter methylene chains, *trans*-**1f,g** (ca. 0.00057 M), and Grubbs first generation catalyst (12.4 mol % or 4.1 mol % per C═C) were refluxed. The crude reaction mixtures were filtered through alumina and then treated with H_2 (5 bar) and PtO_2 (5 mol %) at 50 °C. In each case, two monoplatinum products could be isolated by silica gel column chromatography, *trans*-**2f,g** and *trans*-**2′f,g**. These paralleled those obtained in the earlier work in Scheme 1. However, with *trans*-**2f** and *trans*-**2′f**, the latter dominated (3% vs 25%). This represents the first time a complex derived from *intra*ligand *and inter*ligand metathesis has preferentially formed from a non-octahedral educt.

Careful efforts to detect other monoplatinum products were unsuccessful.[32] Thus, the low mass balance was presumed to reflect the formation of oligomers and polymers, which would be retained on the column. The structures of *trans*-**2′f,g** were evidenced by a diagnostic pattern of ^{13}C NMR signals (two sets of $n/2$ signals in a ca. 2:1 area ratio) and supported by the crystal structures of their *cis* isomers below. Readers are referred to earlier papers for analyses of additional NMR properties.[16,17,23]

An analogous reaction sequence for the complex with the longest methylene chain, *trans*-**2k**, is presented in Scheme 5 (top). However, analogous products were not obtained. Rather, a single monoplatinum adduct could be isolated in 39% yield.

DOI: 10.1021/acs.organomet.8b00345
Organometallics 2018, 37, 2991−3000

Scheme 4. Syntheses of Title Complexes with n = 20 and 22

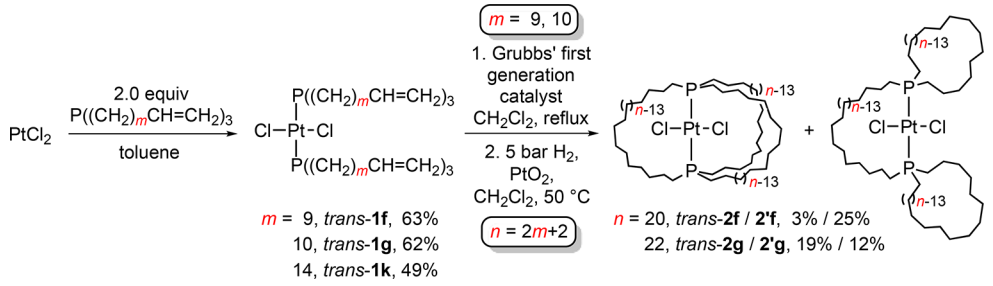

Scheme 5. Syntheses of Title Complexes with n = 30

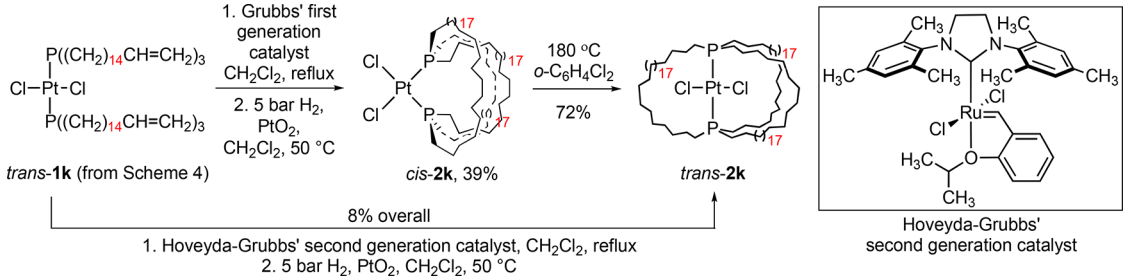

It exhibited a much larger $^{1}J_{PPt}$ value (3530 vs 2389−2307 Hz), suggesting a *cis* coordination geometry and the parachute-like complex *cis*-**2k**, as proven by additional experiments below. This result was reproduced by two co-workers several times (although in one case, a minor coproduct was detected).

Given the thermodynamic relationships established below, this requires a species on the *trans*-**1k** to *cis*-**2k** reaction coordinate that is more stable as a *cis* isomer (in CH_2Cl_2) and an accessible mechanism for isomerization. Thus, a $^{31}P\{^{1}H\}$ NMR spectrum of the soluble crude metathesis product prior to hydrogenation was recorded ($CDCl_3$; Figure S2, Supporting Information). As usual, numerous signals were observed, with some presumably reflecting a distribution of E/Z C=C isomers. These included two prominent singlets at 1.5 and 2.5 ppm and a cluster near 5.5 ppm. Based upon chemical shift trends,[34] the last group can be confidently assigned to *trans* P−Pt−P isomers and the first singlet to a *cis* P−Pt−P isomer.

When analogous experiments were conducted, but $^{31}P\{^{1}H\}$ NMR spectra were recorded prior to complete metathesis, there were additional signals in the 1.5 ppm region, consistent with the presence of *cis*-**1k** (Figure S1). However, in no spectra were any platinum satellites ($^{1}J_{PPt}$) resolved. When *trans*-**1k** was subjected to the initial conditions in Scheme 5, but in the absence of Grubbs catalyst, it was recovered unchanged. However, some *cis*-**1k** could be detected after weeks at room temperature (vide infra).

The interconversion of *cis*/*trans* isomers of platinum(II) complexes is known to be catalyzed by both phosphines and anions,[35−37] either of which can be supplied by Grubbs first generation catalyst. Although Hoveyda−Grubbs-type catalysts have always given inferior preparative results in ring-closing metatheses of the types in Scheme 1, the NHC containing second generation version lacks a phosphine ligand. Accordingly, a parallel sequence was conducted as shown in Scheme 5 (bottom). Now *trans*-**2k** was exclusively obtained, albeit in only 8% yield. Additional analyses are provided in the discussion section.

Thermal Equilibrations. In order to provide context for the first step in Scheme 5, various thermolyses were carried out, with the goal of effecting equilibrations. First, an *o*-$C_6H_4Cl_2$ (*o*-dichlorobenzene) solution of *cis*-**2k** was kept at 180 °C and monitored by $^{31}P\{^{1}H\}$ NMR. Clean isomerization to gyroscope-like *trans*-**2k**—the product initially expected in Scheme 5—was observed. Workup after 48 h gave *trans*-**2k** in 72% yield ($^{1}J_{PPt}$ = 2364 Hz). This result is in line with analogous isomerizations of *cis*-**2c,g** (Scheme 2) to *trans*-**2c,g** reported earlier, as well as extensive gas-phase DFT calculations.[23]

Next, room temperature CH_2Cl_2 solutions of the educts *trans*-**1f,g** were monitored by $^{31}P\{^{1}H\}$ NMR for several months. As shown in Scheme 6 (top) and Figures 1 and 2, 40−60%

Scheme 6. Additional Thermal Isomerizations

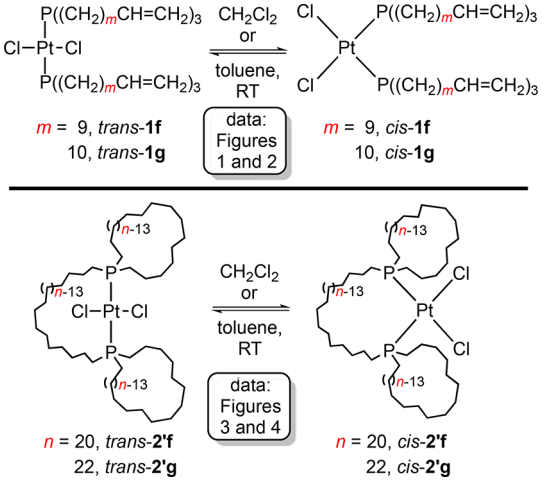

conversions to *cis*-**1f,g**[15,23] (very) gradually occurred. An analogous experiment with *trans*-**1g** in toluene gave only a 9% conversion to *cis*-**1g**. When this sample was kept at 100 °C for 2 days, no further reaction occurred. Hence, it is concluded that the isomerization of *trans*-**1g** is thermodynamically unfavorable in the less polar medium toluene but favorable in the more polar medium CH_2Cl_2. The isomerization of *trans*-**1f** appears slightly unfavorable in CH_2Cl_2, suggesting a modest dependence of the equilibrium upon the methylene chain length.

DOI: 10.1021/acs.organomet.8b00345
Organometallics 2018, 37, 2991−3000

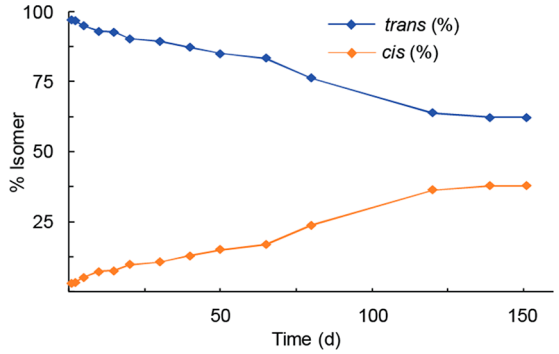

Figure 1. Isomerization of *trans*-**1f** (blue diamond) to *cis*-**1f** (orange diamond) in CH_2Cl_2 at RT (62:38 after 151 days).

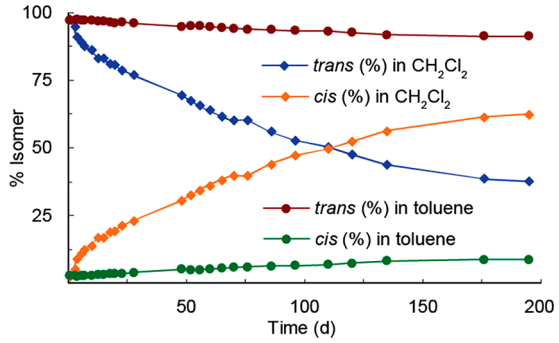

Figure 2. Isomerization of *trans*-**1g** (blue diamond or maroon circle) to *cis*-**1g** (orange diamond or green circle) in CH_2Cl_2 or toluene at RT (39:61 or 91:09 after 195 days).

Analogous experiments were conducted with CH_2Cl_2 and toluene solutions of *trans*-**2′f,g**. As shown in Scheme 6 (bottom) and Figures 3 and 4, 58−56% conversions to *cis*-**2′f,g** were

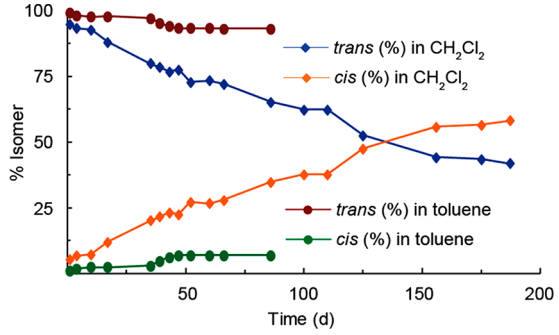

Figure 3. Isomerization of *trans*-**2′f** (blue diamond or maroon circle) to *cis*-**2′f** (orange diamond or green circle) in CH_2Cl_2 or toluene at RT (42:58 or 93:07 after 187 or 86 days).

observed in CH_2Cl_2 but only a 7% conversion to *cis*-**2′f** in toluene. When the last sample was kept at 100 °C for 2 days, no further reaction occurred. The toluene was replaced by *o*-$C_6H_4Cl_2$ and the sample kept at 150 °C for 2 days. Again, no further reaction occurred. Hence, toluene and *o*-$C_6H_4Cl_2$ are insufficiently polar to shift the equilibrium toward the *cis* isomers. These results are in line with gas-phase DFT calculations reported earlier.[23]

Crystal Structures. In view of the potential for interesting structural features, efforts were made to crystallize all of the cyclic compounds in Schemes 4−6. Crystals of a THF solvate of gyroscope-like *trans*-**2g**, and two complexes representing the

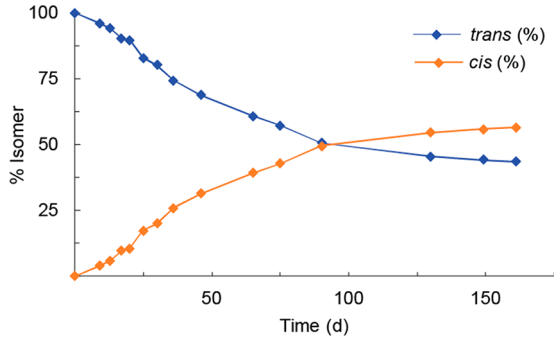

Figure 4. Isomerization of *trans*-**2′g** (blue diamond) to *cis*-**2′g** (orange diamond) in CH_2Cl_2 at RT (44:56 after 161 days).

alternative ring-closing metathesis mode, *cis*-**2′f,g**, were grown, as described in the Experimental Section. X-ray data were collected and the structures solved, as summarized in Table S1 and the Experimental Section. The molecular structures are depicted in Figures 5 and 6. Key bond lengths and angles are given in Table 1.

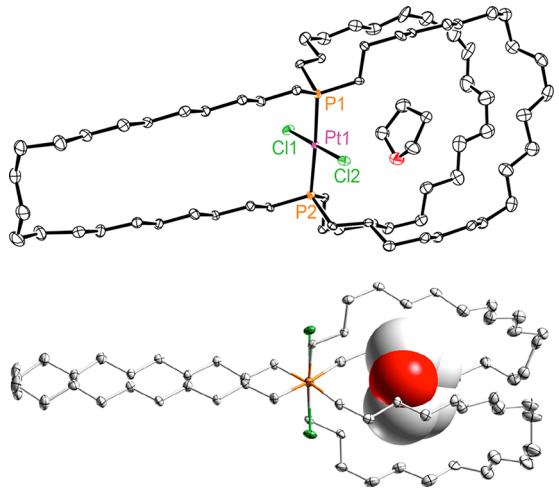

Figure 5. Thermal ellipsoid plot (50% probability) of *trans*-**2g**·THF (top) and view along the P−Pt−P axis (bottom).

Complex *trans*-**2g** represents the gyroscope-like complex with the largest macrocycles (25-membered) that has been structurally characterized to date. The THF molecule is sandwiched between two macrocycles, as opposed to occupying the cavity of only one. The structure illustrates two limiting modes by which increasingly larger macrocycles can fill space. The left most macrocycle in either view can be considered "horizontally extended" with an "all anti" $(CH_2)_9$ segment emanating from each phosphorus atom (torsion angle range 180.0(4) to 169.7(4)°; average 176.5°). The ninth methylene group then initiates a *gauche* C−C−C−C linkage (torsion angles 65.2(6) and 60.6(6)°), several of which are necessary for closing any carbocyclic ring. The other macrocycles extend somewhat in the (vertical) direction of the P−Pt−P axis, as reflected by two Pt−P−C−C linkages with *anti* conformations (torsion angles 178.3(3) and 179.2(3)°). This leads to particularly spacious macrocycle cavities, as seen in the space-filling representation in the toc graphic.

As is evident from Figure 6, *cis*-**2′f,g** adopt quite similar solid state conformations, with several homologous *gauche*/*anti* sequences. Furthermore, both crystallize in the space group

DOI: 10.1021/acs.organomet.8b00345
Organometallics 2018, 37, 2991−3000

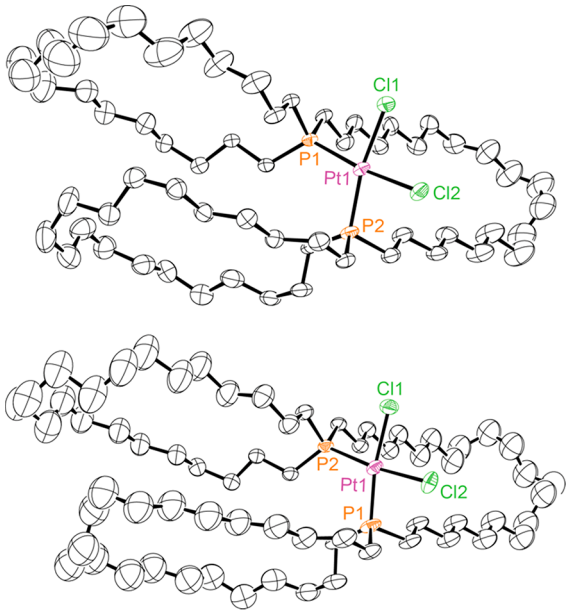

Figure 6. Thermal ellipsoid plots (50% probability) of *cis*-**2′f** (top) and *cis*-**2′g** (bottom).

Table 1. Key Crystallographic Bond Lengths (Å) and Angles (deg)

	trans-**2g**·THF	*cis*-**2′f**	*cis*-**2′g**
Pt−P	2.3100(11)	2.2576(15)	2.251(4)
	2.3199(11)	2.2468(15)	2.263(4)
Pt−Cl	2.3099(11)	2.3717(16)	2.367(4)
	2.3125(11)	2.3590(16)	2.359(4)
P−Pt−P	177.06(4)	103.90(6)	104.35(14)
P−Pt−Cl	93.97(4)	84.93(6)	83.59(16)
	86.29(4)	84.16(6)	84.31(13)
	85.91(4)	171.62(6)	170.67(15)
	93.86(4)	169.94(6)	172.03(14)
Cl−Pt−Cl	179.59(5)	87.25(6)	87.81(15)

$P2_1/c$ with $Z = 4$. Accordingly, the unit cell dimensions are similar, with the volume of the former being slightly smaller (6246.7 vs 6798.9 Å^3). The greatest difference is found in the lengths of the *a* axes (24.5316(12) vs 26.533(3) Å), the directions of which nearly coincide with the long dimensions of the roughly elliptical macrocycles in Figure 6.

The bond lengths and angles in Table 1 fall within standard ranges. However, the platinum−phosphorus bonds that are *trans* to phosphorus atoms are distinctly longer than those that are *trans* to chlorine atoms (2.3199(11)−2.3100(11) Å vs 2.263(4)−2.2468(15) Å), and the platinum−chlorine bonds that are *trans* to phosphorus atoms are distinctly longer than those that are *trans* to chlorine atoms (2.3717(16)−2.359(4) Å vs 2.3125(11)−2.3099(11) Å). These trends follow logically from the *trans* influence and are paralleled in other series of related complexes.[38,39]

DISCUSSION

The results in Schemes 4 and 5 establish that an upper limit has not yet been reached with respect to macrocycle sizes in gyroscope-like complexes accessed by three-fold intramolecular alkene metatheses. Extensions beyond the 30 three-membered rings in *trans*-**2k** would seemingly only require α,ω-haloalkene building blocks $X(CH_2)_mCH{=}CH_2$ with $m \geq 14$, for which viable synthetic routes exist.[40,41] This also augurs well for the availability of increasingly larger dibridgehead diphosphines of the type **3** (Scheme 3). In terms of *trans*-**2**/*trans*-**2′** selectivities, the ratios appear highest (considering Schemes 1, 4, and 5 together) when $n/2$ is an odd integer. This curious trend is also evident with octahedral coordination geometries.[21,22]

However, the initial formation of the parachute-like complex *cis*-**2k** (Scheme 5) represents a complication with respect to future extensions. On a positive note, there seems to be a beneficial effect upon yield relative to those of *trans*-**2f,g** in Scheme 4, and the subsequent thermal isomerization to *trans*-**2k** is spectroscopically quantitative. Importantly, the isomerizations of the model compounds in Scheme 6 and Figures 1−4 show that *cis* isomers are generally favored in CH_2Cl_2, with the solvent for the metatheses and hydrogenations in Schemes 4 and 5. However, equilibrations require months at room temperature and should not be appreciably accelerated under the reflux conditions of the metatheses.

The detection of some *cis* adducts among the crude metathesis products, as well as the apparent *trans*/*cis* isomerization of the educt **1k**, supports the well-precedented[35,37] possibility of a phosphine-catalyzed isomerization that can be avoided with the Hoveyda−Grubbs second generation catalyst. This poses the question as to why analogous phenomena are not seen with the reactions in Scheme 1, which in several cases were carefully scrutinized for *cis* products. Although it represents an extrapolation from only two points, the data for *trans*-**1f,g** (Figures 1 and 2) seem to indicate that, in CH_2Cl_2, *trans*-**1** becomes progressively more favored as the methylene chains are shortened.

Grubbs catalyst has often been applied in toluene[42−44] and occasionally in haloarenes.[21−23,45,46] Thus, another test of the preceding interpretation would be to conduct analogous metatheses in these less polar solvents. However, in preliminary experiments, the metathesis with Grubbs first generation catalyst in Scheme 5 was much slower in toluene, even at higher catalyst loadings (conversion still incomplete after 7 days).

Another open question is whether it will prove possible, with increasing methylene chain lengths, to access additional types of isomers, such as the topologically novel species *trans*-**2″** in Scheme 1. As noted above, such chain crossing has now been documented in derivatives of dibridgehead diphosphines **3** that lack P−M−P linkages.[25,26] All that seemingly would be needed are methylene bridges that are sufficiently long to accommodate both a svelte Cl−Pt−Cl moiety and a methylene chain. Toward this end, the macrocycle size in *trans*-**2g** already seems adequate.

However, there are additional considerations. On the reaction coordinate to gyroscope-like complexes *trans*-**2**, the final ring-closing step involves the bicyclic intermediate **I** with *syn* $(CH_2)_mCH{=}CH_2$ chains shown in Figure 7. In contrast, the final ring-closing step en route to *trans*-**2″** may entail the bicyclic intermediate **II**, with "mismatched" *anti* $(CH_2)_mCH{=}CH_2$ chains. This insight suggests a more sophisticated synthetic approach, inspired by an earlier synthesis of a related diphosphine complex **III** ($n = 14$) that features two *anti*-pentafluorophenyl groups.[33] The optimum precursor to *trans*-**2″** would be **IV**, in which the aryl groups of **III** have been replaced by $(CH_2)_mCH{=}CH_2$ moieties. A subsequent reaction with Grubbs catalyst is certain to give oligomers, but some amount of *trans*-**2″** would (after hydrogenation) logically be anticipated. The challenge is to realize a viable route to **IV**, possibly from an analogue of **III** with appropriate *anti* P−X groups.

DOI: 10.1021/acs.organomet.8b00345
Organometallics 2018, 37, 2991−3000

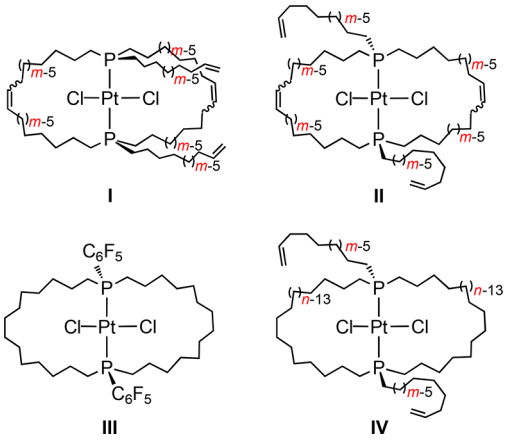

Figure 7. Additional relevant structures.

In summary, this study has greatly expanded the range of *m*/*n* dimensions available to the types of platinum complexes in Schemes 1 and 2. The new monophosphine ligands $P((CH_2)_mCH{=}CH_2)_3$ can also likely be applied to other metals and coordination geometries to yield numerous new gyroscope-like complexes, with enhanced possibilities for topologically novel coproducts. These and related themes will be the subject of future studies from this laboratory.

EXPERIMENTAL SECTION

General. All reactions except hydrogenations were conducted under inert atmospheres using standard Schlenk techniques. Chemicals were treated as follows: hexanes, CH_2Cl_2, toluene, and THF dried and degassed using a Glass Contour solvent purification system; *o*-$C_6H_4Cl_2$, distilled under reduced pressure and degassed; $CDCl_3$ (Cambridge Isotope Laboratories), magnesium turnings (Aldrich, 98%), anhydrous $PtCl_2$ (ABCR, 99.9%), PCl_3 (Merck, 99%), NH_4Cl (Mallinckrodt Chemicals, 99.9%), Grubbs first generation catalyst $((Cy_3P)_2Ru(=CHPh)Cl_2$; Aldrich, 97%), Hoveyda−Grubbs second generation catalyst $((H_2IMes)Ru(=CHC_6H_4(o\text{-}OCH(CH_3)_2)Cl_2$, H_2IMes = 1,3-dimesityl-4,5-dihydroimidazol-2-ylidene; Aldrich, 97%), PtO_2 (Aldrich, 99.9%), 16-bromo-1-hexadecene (Amadis Chemical, 95%), SiO_2 (Silicycle), and neutral Al_2O_3 (Macherey-Nagel), used as received.

NMR spectra were recorded on a Varian NMRS 500 MHz instrument at ambient probe temperatures and referenced as follows (δ, ppm): ^1H, residual internal $CHCl_3$ (7.26); $^{13}C\{^1H\}$, internal $CDCl_3$ (77.16); $^{31}P\{^1H\}$, external H_3PO_4 (0.00). IR spectra were recorded on a Shimadzu IRAffinity-1 spectrometer with a Pike MIRacle ATR system (diamond/ZnSe crystal). Melting points were recorded using a Stanford Research Systems MPA100 (OptiMelt) automated apparatus. Microanalyses were conducted by Atlantic Microlab, Inc.

$P((CH_2)_{10}CH{=}CH_2)_3$. A round-bottom flask was charged with $Br(CH_2)_{10}CH{=}CH_2$ (5.014 g, 20.3 mmol)[47] and degassed (3 × freeze−pump−thaw). THF (25 mL) was added, the mixture was cooled to 0 °C, and magnesium turnings (0.984 g, 40.5 mmol) were added with stirring. After 1 h, the cooling bath was removed. The mixture was stirred overnight and then filtered (glass frit). The filtrate was cooled to 0 °C. A solution of PCl_3 (0.49 mL, 5.6 mmol) in THF (10 mL) was added dropwise via syringe over 5 min. After 1 h, the cooling bath was removed. The mixture was stirred overnight and again cooled to 0 °C. Aqueous NH_4Cl (20 mL) was added dropwise over 5 min. After 1 h, the cooling bath was removed. The mixture was stirred for 2 h and the colorless aqueous phase removed via syringe. The solvent was removed from the organic phase by rotary evaporation, and CH_2Cl_2 (10 mL) was added. The solution was filtered under a nitrogen atmosphere through a short pad of silica gel (5 × 3 cm), which was washed with CH_2Cl_2 (100 mL). The solvent was removed by oil pump vacuum to give $P((CH_2)_{10}CH{=}CH_2)_3$ (2.036 g, 3.82 mmol, 68%) as a greenish yellow oil.

NMR ($CDCl_3$, δ/ppm): ^1H (500 MHz) 5.80 (ddt, 3H, $^3J_{HHtrans}$ = 17.0 Hz, $^3J_{HHcis}$ = 10.1 Hz, $^3J_{HH}$ = 6.8 Hz, $CH{=}$), 4.98 (br d, 3H, $^3J_{HHtrans}$ = 17.1 Hz, $=CH_EH_Z$), 4.92 (br d, 3H, $^3J_{HHcis}$ = 10.2 Hz, $=CH_EH_Z$), 2.07−1.99 (m, 6H, $CH_2CH{=}$), 1.45−1.21 (m, 54H, remaining CH_2); $^{13}C\{^1H\}$[48] (126 MHz) 139.0 (s, $CH{=}$), 114.0 (s, $=CH_2$), 33.8 (s, $CH_2CH{=}$), 31.4 (d, $^3J_{CP}$ = 10.6 Hz, $PCH_2CH_2CH_2$), 29.53 (s, CH_2), 29.48 (s, CH_2), 29.4 (s, CH_2), 29.3 (s, CH_2), 29.1 (s, CH_2), 28.9 (s, CH_2), 27.2 (d, $^2J_{CP}$ = 12.4 Hz, PCH_2CH_2), 25.8 (d, $^1J_{CP}$ = 12.6 Hz, PCH_2); $^{31}P\{^1H\}$ (202 MHz) −31.0 (s).

$P((CH_2)_{14}CH{=}CH_2)_3$. THF (30 mL), $Br(CH_2)_{14}CH{=}CH_2$ (7.085 g, 23.3 mmol), magnesium turnings (1.162 g, 48.4 mmol), a solution of PCl_3 (0.56 mL, 6.46 mmol) in THF (10 mL), and aqueous NH_4Cl (20 mL) were combined in a procedure analogous to that given for $P((CH_2)_{10}CH{=}CH_2)_3$. An identical workup gave $P((CH_2)_{14}CH{=}CH_2)_3$ (2.090 g, 4.13 mmol, 64%) as a greenish yellow oil.

NMR ($CDCl_3$, δ/ppm): ^1H (500 MHz) 5.83 (ddt, 3H, $^3J_{HHtrans}$ = 17.0 Hz, $^3J_{HHcis}$ = 10.3 Hz, $^3J_{HH}$ = 6.7 Hz, $CH{=}$), 5.00 (br d, 3H, $^3J_{HHtrans}$ = 17.0 Hz, $=CH_EH_Z$), 4.94 (br d, 3H, $^3J_{HHcis}$ = 10.8 Hz, $=CH_EH_Z$), 2.09−2.01 (m, 6H, $CH_2CH{=}$), 1.46−1.20 (m, 78H, remaining CH_2); $^{13}C\{^1H\}$[48] (126 MHz) 139.2 (s, $CH{=}$), 114.1 (s, $=CH_2$), 33.8 (s, $CH_2CH{=}$), 31.5 (d, $^3J_{CP}$ = 10.3 Hz, $PCH_2CH_2CH_2$), 29.70 (s, CH_2), 29.69 (s, 2 × CH_2), 29.64 (s, CH_2), 29.58 (s, CH_2), 29.5 (s, CH_2), 29.41 (s, CH_2), 29.37 (s, CH_2), 29.17 (s, CH_2), 29.0 (s, CH_2), 27.2 (d, $^2J_{CP}$ = 11.6 Hz, PCH_2CH_2), 25.9 (d, $^1J_{CP}$ = 12.6 Hz, PCH_2); $^{31}P\{^1H\}$ (202 MHz) −25.7 (s).

***trans*-$PtCl_2(P((CH_2)_9CH{=}CH_2)_3)_2$ (*trans*-1f).** A Schlenk flask was charged with $P((CH_2)_9CH{=}CH_2)_3$ (1.596 g, 3.25 mmol),[15] toluene (10 mL), and $PtCl_2$ (0.433 g, 1.63 mmol) with stirring. After 48 h, the mixture was concentrated to ca. 2 mL and placed at the top of a silica column (3.5 × 20 cm), which was eluted with hexanes/CH_2Cl_2 (90:10 to 80:20 v/v) and then CH_2Cl_2. The solvent was removed from the product fractions by oil pump vacuum to give *trans*-**1f** (0.821 g, 1.02 mmol, 63%) as a pale yellow oil. Anal. Calcd (%) for $C_{66}H_{126}Cl_2P_2Pt$ (1247.67): C, 63.54; H, 10.18; found C, 63.80; H, 10.34.

NMR ($CDCl_3$, δ/ppm): ^1H (500 MHz) 5.80 (ddt, 6H, $^3J_{HHtrans}$ = 17.0 Hz, $^3J_{HHcis}$= 10.2 Hz, $^3J_{HH}$ = 6.7 Hz, $CH{=}$), 4.99 (br d, 6H, $^3J_{HHtrans}$= 17.1 Hz, $=CH_EH_Z$), 4.92 (br d, 6H, $^3J_{HHcis}$ = 10.3 Hz, $=CH_EH_Z$), 2.09−1.98 (m, 12H, $CH_2CH{=}$), 1.87−1.77 (br m, 12H, PCH_2), 1.60−1.51 (br m, 12H, PCH_2CH_2), 1.45−1.21 (m, 72H, remaining CH_2); $^{13}C\{^1H\}$[48] (126 MHz) 139.2 (s, $CH{=}$), 114.1 (s, $=CH_2$), 33.8 (s, $CH_2CH{=}$), 31.2 (virtual t,[50] $^3J_{CP}$ = 6.48 Hz, $PCH_2CH_2CH_2$), 29.5 (s, 2 × CH_2), 29.22 (s, CH_2), 29.15 (s, CH_2), 28.9 (s, CH_2), 23.7 (s, PCH_2CH_2), 20.4 (virtual t,[50] $^1J_{CP}$ = 16.3 Hz, PCH_2); $^{31}P\{^1H\}$ (202 MHz) 5.09 (s, J_{PPt} = 2375 Hz[51]); IR (cm^{-1}, powder film) 2924 (s), 2855 (m), 1458 (m), 718 (m).

***trans*-$PtCl_2(P((CH_2)_{10}CH{=}CH_2)_3)_2$ (*trans*-1g).** Toluene (10 mL), $P((CH_2)_{10}CH{=}CH_2)_3$ (1.529 g, 2.87 mmol), and $PtCl_2$(0.382 g, 1.44 mmol) were combined in a procedure analogous to that for *trans*-**1f**. An identical workup gave *trans*-**1g** (1.186 g, 0.891 mmol, 62%) as a pale yellow oil. Anal. Calcd (%) for $C_{72}H_{138}Cl_2P_2Pt$ (1331.83): C, 64.93; H, 10.44; found C, 65.21; H, 10.54.

NMR ($CDCl_3$, δ/ppm): ^1H (500 MHz) 5.79 (ddt, 6H, $^3J_{HHtrans}$ = 17.0 Hz, $^3J_{HHcis}$ = 10.1 Hz, $^3J_{HH}$ = 6.7 Hz, $CH{=}$), 4.98 (br d, 6H, $^3J_{HHtrans}$ = 17.1 Hz, $=CH_EH_Z$), 4.91 (br d, 6H, $^3J_{HHcis}$ = 10.3 Hz, $=CH_EH_Z$), 2.06−1.99 (m, 12H, $CH_2CH{=}$), 1.87−1.77 (br m, 12H, PCH_2), 1.59−1.50 (br m, 12H, PCH_2CH_2), 1.45−1.33 (m, 24H, 2 × CH_2), 1.32−1.20 (m, 60H, remaining CH_2); $^{13}C\{^1H\}$[48] (126 MHz) 139.1 (s, $CH{=}$), 114.1 (s, $=CH_2$), 33.8 (s, $CH_2CH{=}$), 31.2 (virtual t,[50] $^3J_{CP}$ = 6.5 Hz, $PCH_2CH_2CH_2$), 29.6 (s, CH_2), 29.5 (s, 2 × CH_2), 29.22 (s, CH_2), 29.17 (s, CH_2), 28.9 (s, CH_2), 23.6 (s, PCH_2CH_2), 20.4 (virtual t,[50] $^1J_{CP}$ = 16.1 Hz, PCH_2); $^{31}P\{^1H\}$ (202 MHz) 4.69 (s, $^1J_{PPt}$ = 2382 Hz[51]); IR (cm^{-1}, powder film) 2924 (s), 2847 (m), 1458 (m), 718 (m).

***trans*-$PtCl_2(P((CH_2)_{14}CH{=}CH_2)_3)_2$ (*trans*-1k).** Toluene (10 mL), $P((CH_2)_{14}CH{=}CH_2)_3$ (1.614 g, 2.30 mmol), and $PtCl_2$(0.3061 g, 1.151 mmol) were combined in a procedure analogous to that for *trans*-**1f**. An identical workup gave *trans*-**1k** (0.941 g, 0.564 mmol, 49%) as a light yellow solid, mp (capillary) 57 °C. Anal. Calcd (%) for $C_{96}H_{186}Cl_2P_2Pt$ (1668.48): C, 69.11; H, 11.24; found C, 69.12; H, 11.41.

DOI: 10.1021/acs.organomet.8b00345
Organometallics 2018, 37, 2991−3000

NMR ($CDCl_3$, δ/ppm): ^{1}H (500 MHz) 5.82 (ddt, 6H, $^3J_{HHtrans}$ = 17.0 Hz, $^3J_{HHcis}$ = 10.1 Hz, $^3J_{HH}$ = 6.6 Hz, C*H*═), 5.00 (br d, 6H, $^3J_{HHtrans}$ = 17.1 Hz, ═CH$_E$*H*$_Z$), 4.93 (br d, 6H, $^3J_{HHcis}$ = 10.9 Hz, ═C*H*$_E$H$_Z$), 2.09−2.01 (m, 12H, C*H*$_2$CH═), 1.88−1.80 (m, 12H, PC*H*$_2$), 1.61−1.52 (m, 12H, PCH$_2$C*H*$_2$), 1.45−1.35 (m, 24H, C*H*$_2$), 1.34−1.20 (m, 108H, remaining C*H*$_2$); ^{13}C{^{1}H}[48] (126 MHz) 139.2 (s, CH═), 114.1 (s, ═CH$_2$), 33.8 (s, CH$_2$CH═), 31.2 (virtual t,[50] $^3J_{CP}$ = 6.5 Hz, PCH$_2$CH$_2$CH$_2$), 29.71 (s, 2 × CH$_2$), 29.74 (s, 2 × CH$_2$), 29.67 (s, CH$_2$), 29.58 (s, CH$_2$), 29.56 (s, CH$_2$), 29.3 (s, CH$_2$), 29.2 (s, CH$_2$), 27.0 (s, CH$_2$), 23.7 (s, PCH$_2$CH$_2$), 20.4 (virtual t,[50] $^1J_{CP}$ = 16.1 Hz, PCH$_2$); ^{31}P{^{1}H} (202 MHz) 4.69 (s, J_{PPt} = 2379 Hz[51]); IR (cm^{-1}, powder film) 2916 (s), 2850 (m), 1465 (m), 911 (m), 717 (m).

***trans*-PtCl$_2$(P(CH$_2$)$_{20}$)$_3$P) (*trans*-2f) and *trans*-PtCl$_2$-(P((CH$_2$)$_{19}$CH$_2$)(CH$_2$)$_{20}$P((CH$_2$)$_{19}$CH$_2$)) (*trans*-2′f).** A Schlenk flask was charged with *trans*-**1f** (0.545 g, 0.437 mmol), Grubbs first generation catalyst (0.0444 g, 0.054 mmol, 12.4 mol %), and CH_2Cl_2 (750 mL; the resulting solution is 0.00058 M in *trans*-**1f**) and fitted with a condenser. The solution was refluxed with stirring (48 h). The solvent was removed by oil pump vacuum, and CH_2Cl_2 was added. The sample was passed through a short pad of neutral alumina, rinsing with CH_2Cl_2. A Fischer−Porter bottle was charged with the filtrate (reduced to 20 mL), PtO_2 (0.0200 g, 0.088 mmol), and H_2 (5 bar). The mixture was kept at 50 °C (venting H_2 to maintain 5 bar) and stirred (48 h). The solvent was removed by oil pump vacuum. The residue was placed at the top of a silica column (3.5 × 26 cm), which was eluted with hexanes (1000 mL) and then hexanes/CH_2Cl_2 (10:1 to 6:1 v/v). The solvent was removed from the product fractions by rotary evaporation to give *trans*-**2f** (0.0175 g, 0.015 mmol, 3%) and *trans*-**2′f** (0.1263 g, 0.108 mmol, 25%) as pale yellow waxy oils that solidified after 48−72 h.

Data for *trans*-**2f**: mp 47 °C (capillary). Anal. Calcd (%) for $C_{60}H_{120}Cl_2P_2Pt$ (1169.55): C, 61.62; H, 10.34; found C, 61.40; H, 10.40.

NMR ($CDCl_3$, δ/ppm): ^{1}H (500 MHz) 1.90−1.75 (m, 12H, PC*H*$_2$), 1.70−1.58 (m, 12H, PCH$_2$C*H*$_2$), 1.50−1.38 (m, 12H, PCH$_2$CH$_2$C*H*$_2$), 1.38−1.19 (m, 84H, remaining C*H*$_2$); ^{13}C{^{1}H}[48] (126 MHz) 30.9 (virtual t,[50] $^3J_{CP}$ = 6.8 Hz, PCH$_2$CH$_2$CH$_2$), 28.9 (s, CH$_2$), 28.71 (s, CH$_2$), 28.66 (s, CH$_2$), 28.46 (s, CH$_2$), 28.45 (s, CH$_2$), 28.1 (s, CH$_2$), 28.0 (s, CH$_2$), 23.6 (s, PCH$_2$CH$_2$), 20.6 (virtual t,[50] $^1J_{CP}$ = 16.2 Hz, PCH$_2$); ^{31}P{^{1}H} (202 MHz) 5.06 (s, $^1J_{PPt}$ = 2307 Hz[51]); IR (cm^{-1}, powder film) 2916 (s), 2847 (m), 1458 (m), 718 (m).

Data for *trans*-**2′f**: mp 66 °C (capillary). Anal. Calcd (%) for $C_{60}H_{120}Cl_2P_2Pt$ (1169.55): C, 61.62; H, 10.34; found C, 61.89; H, 10.46.

NMR ($CDCl_3$, δ/ppm): ^{1}H (500 MHz) 2.06−1.89 (m, 6H, PC*H*$_2$), 1.88−1.53 (m, 24H, PCH$_2$C*H*$_2$C*H*$_2$), 1.52−1.21 (m, 90H, remaining C*H*$_2$); ^{13}C{^{1}H}[48] (126 MHz) 31.2 (virtual t,[50] $^3J_{CP}$ = 6.8 Hz, PCH$_2$CH$_2$CH$_2$), 30.7 (virtual t,[50] $^3J_{CP}$ = 6.3 Hz, 2PCH$_2$CH$_2$CH$_2$), 29.24 (s, CH$_2$), 29.17 (s, CH$_2$), 28.9 (s, 2CH$_2$), 28.8 (s, CH$_2$), 28.5 (s, 2 × 2CH$_2$), 28.3 (s, CH$_2$/2CH$_2$), 28.1 (s, 2CH$_2$), 28.01 (s, 2CH$_2$), 27.97 (s, CH$_2$), 27.6 (s, 2CH$_2$), 27.4 (s, CH$_2$), 27.3 (s, CH$_2$), 24.5 (s, PCH$_2$CH$_2$), 23.0 (s, 2PCH$_2$CH$_2$), 22.2 (virtual t,[50] $^1J_{CP}$ = 16.4 Hz, PCH$_2$), 19.3 (virtual t,[50] $^1J_{CP}$ = 16.3 Hz, 2PCH$_2$); ^{31}P{^{1}H} (202 MHz) 4.93 (s, $^1J_{PPt}$ = 2375 Hz[51]); IR (cm^{-1}, powder film) 2916 (s), 2844 (m), 1459 (m), 716 (m).

***trans*-PtCl$_2$(P(CH$_2$)$_{22}$)$_3$P) (*trans*-2g) and *trans*-PtCl$_2$-(P((CH$_2$)$_{21}$CH$_2$)(CH$_2$)$_{22}$P((CH$_2$)$_{21}$CH$_2$)) (*trans*-2′g).** Grubbs first generation catalyst (0.0427 g, 0.052 mmol, 12.4 mol %), *trans*-**1g** (0.557 g, 0.418 mmol), CH_2Cl_2 (750 mL; the resulting solution is 0.00056 M in *trans*-**1g**), PtO_2 (0.0201 g, 0.088 mmol), and H_2 (5 bar) were combined in a procedure analogous to that given for *trans*-**2f** and *trans*-**2′f**. An identical workup gave *trans*-**2g** (0.1015 g, 0.081 mmol, 19%) and *trans*-**2′g** (0.0652 g, 0.052 mmol, 12%) as pale yellow oils that solidified after 48−72 h.

Data for *trans*-**2g**: mp 47 °C (capillary). Anal. Calcd (%) for $C_{66}H_{132}Cl_2P_2Pt$ (1253.71): C, 63.23; H, 10.61; found C, 63.53; H, 10.77.

NMR ($CDCl_3$, δ/ppm): ^{1}H (500 MHz) 1.88−1.80 (br m, 12H, PC*H*$_2$), 1.63−1.55 (br m, 12H, PCH$_2$C*H*$_2$), 1.45−1.39 (br m, 12H, PCH$_2$CH$_2$C*H*$_2$), 1.36−1.24 (br m, 96H, remaining C*H*$_2$); ^{13}C{^{1}H}[48] (126 MHz) 31.1 (virtual t,[50] $^3J_{CP}$ = 6.6 Hz, PCH$_2$CH$_2$CH$_2$), 29.2 (s, CH$_2$), 29.0 (s, CH$_2$), 28.91 (s, CH$_2$), 28.88 (s, CH$_2$), 28.7 (s, CH$_2$), 28.4 (s, CH$_2$), 28.3 (s, CH$_2$), 28.1 (s, CH$_2$), 23.7 (s, PCH$_2$CH$_2$), 20.6 (virtual t,[50] $^1J_{CP}$ = 16.2 Hz, PCH$_2$); ^{31}P{^{1}H} (202 MHz) 4.85 (s, $^1J_{PPt}$ = 2389 Hz[51]); IR (cm^{-1}, powder film) 2916 (s), 2847 (m), 1458 (m), 718 (m).

Data for *trans*-**2′g**: mp 53 °C (capillary). Anal. Calcd (%) for $C_{66}H_{132}Cl_2P_2Pt$ (1253.71): C, 63.23; H, 10.61; found C, 63.46; H, 10.78.

NMR ($CDCl_3$, δ/ppm): ^{1}H (500 MHz) 2.01−1.90 (m, 6H, PC*H*$_2$), 1.82−1.75 (m, 6H, PC*H*$_2$), 1.68−1.54 (m, 12H, PCH$_2$C*H*$_2$), 1.47−1.37 (m, 12H, PCH$_2$CH$_2$C*H*$_2$), 1.30−1.22 (m, 96H, remaining C*H*$_2$); ^{13}C{^{1}H}[48] (126 MHz) 31.2 (virtual t,[50] $^3J_{CP}$ = 6.76 Hz, PCH$_2$CH$_2$CH$_2$), 30.8 (virtual t,[50] $^3J_{CP}$ = 6.76 Hz, 2PCH$_2$CH$_2$CH$_2$), 29.31 (s, CH$_2$), 29.25 (s, CH$_2$), 29.2 (s, CH$_2$), 29.1 (s, 2CH$_2$), 28.91 (s, CH$_2$), 28.86 (s, 2CH$_2$), 28.64 (s, 2 × 2CH$_2$), 28.63 (s, 2CH$_2$), 28.48 (s, CH$_2$), 28.45 (s, 2CH$_2$), 28.1 (s, 2CH$_2$), 28.0 (s, CH$_2$), 27.91 (s, CH$_2$), 27.88 (s, 2CH$_2$), 27.5 (s, CH$_2$), 24.3 (s, PCH$_2$CH$_2$), 23.0 (s, 2PCH$_2$CH$_2$), 22.0 (virtual t,[50] $^1J_{CP}$ = 16.6 Hz, PCH$_2$), 19.4 (virtual t,[50] $^1J_{CP}$ = 16.6 Hz, 2PCH$_2$); ^{31}P{^{1}H} (202 MHz) 4.85 (s, $^1J_{PPt}$ = 2369 Hz[51]); IR (cm^{-1}, powder film) 2916 (s), 2847 (m), 1458 (m), 718 (m).

***cis*-PtCl$_2$(P(CH$_2$)$_{30}$)$_3$P) (*cis*-2k).** Grubbs first generation catalyst (0.0138 g, 0.017 mmol, 8.9 mol %), *trans*-**1k** (0.3125 g, 0.187 mmol), CH_2Cl_2 (600 mL; the resulting solution is 0.00031 M in *trans*-**1k**), PtO_2 (0.0164 g, 0.072 mmol), and H_2 (5 bar) were combined in a procedure analogous to that given for *trans*-**2f**. An identical workup gave *cis*-**2k** (0.1159 g, 0.073 mmol, 39%) as a white solid, mp (capillary) 153.6 °C. Anal. Calcd (%) for $C_{90}H_{180}Cl_2P_2Pt$ (1590.36): C, 67.97; H, 11.41; found C, 67.88; H, 11.53.

NMR ($CDCl_3$, δ/ppm): ^{1}H (500 MHz) 2.05−2.91 (m, 12H, PC*H*$_2$), 1.60−1.50 (m, 12H, PCH$_2$C*H*$_2$), 1.46−1.37 (m, 12H, PCH$_2$CH$_2$C*H*$_2$), 1.34−1.21 (m, 144H, remaining C*H*$_2$); ^{13}C{^{1}H}[48] (126 MHz) 31.2 (virtual t,[50] $^3J_{CP}$ = 7.1 Hz, 4C, PCH$_2$CH$_2$CH$_2$), 29.70 (s, CH$_2$), 29.65 (s, CH$_2$), 29.6 (s, 2 × CH$_2$), 29.5 (s, CH$_2$), 29.4 (s, CH$_2$), 29.3 (s, CH$_2$), 29.0 (s, CH$_2$), 28.8 (s, CH$_2$), 28.6 (s, CH$_2$), 28.4 (s, CH$_2$), 28.2 (s, CH$_2$), 24.8 (br s, PCH$_2$CH$_2$), 24.6 (br s, PCH$_2$); ^{31}P{^{1}H} (202 MHz) 1.8 (s, $^1J_{PPt}$ = 3530 Hz[51]); IR (cm^{-1}, powder film) 2916 (s), 2850 (m), 1465 (m), 717 (m).

***trans*-PtCl$_2$(P(CH$_2$)$_{30}$)$_3$P)(*trans*-2k). A:** A Schlenk flask was charged with *cis*-**2k** (0.0685 g, 0.043 mmol) and *o*-$C_6H_4Cl_2$ (10 mL) and heated to 180 °C. The isomerization was monitored by ^{31}P{^{1}H} NMR. After 48 h, conversion was complete. The solvent was removed by oil pump vacuum. The residue was chromatographed (silica column, 3 × 20 cm, 6:1 v/v hexanes/CH_2Cl_2). The solvent was removed from the product fractions by rotary evaporation and oil pump vacuum to give *trans*-**2k** as a pale yellow waxy oil, which solidified after 24 h (0.0495 g, 0.031 mmol, 72%): mp (capillary) 46 °C. Anal. Calcd (%) for $C_{90}H_{180}Cl_2P_2Pt$ (1590.36): C, 67.97; H, 11.41; found C, 67.83; H, 11.58. **B:** A Schlenk flask was charged with *trans*-**1k** (0.5382 g, 0.323 mmol), the Hoveyda−Grubbs second generation catalyst (0.0255 g, 0.041 mmol, 12.7 mol %), and CH_2Cl_2 (750 mL; the resulting solution is 0.00043 M in *trans*-**1k**) and fitted with a condenser. The solution was refluxed with stirring (48 h). The solvent was removed by oil pump vacuum, and CH_2Cl_2 was added. The sample was passed through a short pad of neutral alumina, rinsing with CH_2Cl_2. A Fischer−Porter bottle was charged with the filtrate (reduced to 20 mL), PtO_2 (0.0186 g, 0.082 mmol), and H_2 (5 bar). The mixture was kept at 50 °C (venting H_2 to maintain 5 bar) and stirred (48 h). The solvent was removed by oil pump vacuum. The residue was placed at the top of a silica column (3.5 × 26 cm), which was eluted with hexanes (1000 mL) and then hexanes/CH_2Cl_2 (10:1 to 6:1 v/v). The solvent was removed from the product fractions by rotary evaporation to give *trans*-**2k** (0.0411 g, 0.026 mmol, 8%) as a pale yellow waxy oil that solidified after 48−72 h.

NMR ($CDCl_3$, δ/ppm): ^{1}H (500 MHz) 1.89−1.80 (m, 12H, PC*H*$_2$), 1.62−1.53 (m, 12H, PCH$_2$C*H*$_2$), 1.46−1.39 (m, 12H, PCH$_2$CH$_2$C*H*$_2$), 1.36−1.23 (m, 144H, remaining C*H*$_2$); ^{13}C{^{1}H}[48] (126 MHz) 31.2 (virtual t,[50] $^3J_{CP}$ = 6.8 Hz, PCH$_2$CH$_2$CH$_2$), 29.6 (s, 2 × CH$_2$), 29.54 (s, CH$_2$), 29.48 (s, CH$_2$), 29.34 (s, CH$_2$), 29.28 (s, CH$_2$), 29.2 (s, CH$_2$),

DOI: 10.1021/acs.organomet.8b00345
Organometallics 2018, 37, 2991−3000

29.1 (s, CH_2), 29.0 (s, CH_2), 28.8 (s, CH_2), 28.72 (s, CH_2), 28.65 (s, CH_2), 23.7 (s, PCH_2CH_2), 20.5 (virtual t,[50] $^1J_{CP}$ = 16.2 Hz, PCH_2); $^{31}P\{^1H\}$ (202 MHz) 4.73 (s, $^1J_{PPt}$ = 2364 Hz[51]); IR (cm^{-1}, powder film) 2916 (s), 2847 (m), 1458 (m), 718 (m).

Equilibration Experiments. The following are representative. **A** (Figure 2): An NMR tube was charged with *trans*-**1g** (0.0065 g, 0.0049 mmol) and CH_2Cl_2 (0.7 mL). $^{31}P\{^1H\}$ NMR spectra were periodically recorded (after 195 days, δ/ppm): 4.99 (s, $^1J_{PPt}$ = 2382 Hz,[51] *trans*-**1g**, 39%), 0.96 (s, $^1J_{PPt}$ = 3515 Hz,[51] *cis*-**1g**, 61%). **B** (Figure 2): An NMR tube was charged with *trans*-**1g** (0.0064 g, 0.0048 mmol) and toluene (0.7 mL). $^{31}P\{^1H\}$ NMR spectra were periodically recorded (after 195 days, δ/ppm): 5.21 (s, $^1J_{PPt}$ = 2385 Hz,[51] *trans*-**1g**, 91%), 1.18 (s, $^1J_{PPt}$ = 3518 Hz,[51] *cis*-**1g**, 9%). The tube was kept at 100 °C for 2 d. The sample was cooled, and $^{31}P\{^1H\}$ NMR spectra were recorded (δ/ppm): 5.21 (s, $^1J_{PPt}$ = 2380 Hz,[51] *trans*-**1g**, 91%), 1.18 (s, $^1J_{PPt}$ = 3513 Hz,[51] *cis*-**1g**, 9%). **C** (Figure 3): An NMR tube was charged with *trans*-**2′f** (0.0059 g, 0.0050 mmol) and toluene (0.7 mL). $^{31}P\{^1H\}$ NMR spectra were periodically recorded (after 86 days, δ/ppm): 4.93 (s, $^1J_{PPt}$ = 2374 Hz,[51] *trans*-**2′f**, 93%), 1.33 (s, $^1J_{PPt}$ = 3515 Hz,[51] *cis*-**2′f**, 7%). The tube was kept at 100 °C for 2 days. The sample was cooled, and $^{31}P\{^1H\}$ NMR spectra were recorded (δ/ppm): 5.20 (s, $^1J_{PPt}$ = 2380 Hz,[51] *trans*-**2′f**, 93%), 1.17 (s, $^1J_{PPt}$ = 3513 Hz,[51] *cis*-**2′f**, 7%). The solvent was removed by rotary evaporation, and *o*-$C_6H_4Cl_2$ (0.7 mL) was added. The tube was kept at 150 °C for 2 days. The sample was cooled, and $^{31}P\{^1H\}$ NMR spectra was recorded (δ/ppm): 5.27 (s, $^1J_{PPt}$ = 2380 Hz,[51] *trans*-**2′f**, 93%), 1.33 (s, $^1J_{PPt}$ = 3514 Hz,[51] *cis*-**2′f**, 7%).

Crystallography. A. A THF solution of *trans*-**2g** was allowed to slowly concentrate. After 7 days, colorless blocks were obtained. Data were collected as outlined in Table S1. Cell parameters were obtained from 45 frames using a 1° scan and refined with 164 010 reflections. Integrated intensity information for each reflection was obtained by reduction of the data frames with the program APEX3.[52] Lorentz and polarization corrections were applied. Data were scaled, and absorption corrections were applied using the program SADABS.[53] The space group was determined from systematic reflection conditions and statistical tests. The structure was refined (weighted least-squares refinement on F^2) to convergence,[54−56] which revealed a THF molecule for each *trans*-**2g** molecule. Olex2[57] was employed for the final data presentation. Non-hydrogen atoms were refined with anisotropic thermal parameters. Hydrogen atoms were fixed in idealized positions using a riding model. Some carbon atoms exhibited elongated thermal ellipsoids, suggesting disorder. For C57−C60, the disorder could be modeled between two positions (occupancy ratio of 61:39); appropriate restraints were used to keep the metrical parameters meaningful. The absence of additional symmetry or voids was confirmed using PLATON (ADDSYM).[58] **B**. A CH_2Cl_2 solution of *trans*-**2′f** was allowed to slowly concentrate. After 16 days, colorless thin plates of *cis*-**2′f** were obtained (NMR spectra showed both isomers in solution). Data were collected (64 049 reflections), and the structure was solved as in **A**. **C**. A CH_2Cl_2 solution of *trans*-**2′g** was allowed to slowly concentrate. After 15 days, colorless plates of *cis*-**2′g** were obtained. Data were collected (123 992 reflections), and the structure was solved as in **A**.

■ ASSOCIATED CONTENT

Supporting Information

The Supporting Information is available free of charge on the ACS Publications website at DOI: 10.1021/acs.organomet.8b00345.

$^{31}P\{^1H\}$ NMR spectra of the crude product from the metathesis step in Scheme 5; ^1H, $^{13}C\{^1H\}$, and $^{31}P\{^1H\}$ NMR spectra of new compounds; table of crystallographic data (PDF)

Accession Codes

CCDC 1834628 and 1834649−1834650 contain the supplementary crystallographic data for this paper. These data can be obtained free of charge via www.ccdc.cam.ac.uk/data_request/cif, or by emailing data_request@ccdc.cam.ac.uk, or by contacting The Cambridge Crystallographic Data Centre, 12 Union Road, Cambridge CB2 1EZ, UK; fax: +44 1223 336033.

■ AUTHOR INFORMATION

Corresponding Author

*E-mail: gladysz@mail.chem.tamu.edu.

ORCID

Sugam Kharel: 0000-0001-6106-4639

Hemant Joshi: 0000-0002-7616-0241

John A. Gladysz: 0000-0002-7012-4872

Author Contributions

†S.K. and H.J. contributed equally to this work.

Notes

The authors declare no competing financial interest.

■ ACKNOWLEDGMENTS

The authors thank the U.S. National Science Foundation (CHE-1566601) for support.

■ REFERENCES

(1) Khuong, T.-A. V.; Nuñez, J. E.; Godinez, C. E.; Garcia-Garibay, M. A. Crystalline Molecular Machines: A Quest Toward Solid-State Dynamics and Function. *Acc. Chem. Res.* **2006**, *39*, 413−422.

(2) Nuñez, J. E.; Natarajan, A.; Khan, S. I.; Garcia-Garibay, M. A. Synthesis of a Triply-Bridged Molecular Gyroscope by a Directed Meridional Cyclization Strategy. *Org. Lett.* **2007**, *9*, 3559−3561.

(3) Vogelsberg, C. S.; Garcia-Garibay, M. A. Crystalline molecular machines: function, phase order, dimensionality, and composition. *Chem. Soc. Rev.* **2012**, *41*, 1892−1910.

(4) Pérez-Estrada, S.; Rodríguez-Molina, B.; Xiao, L.; Santillan, R.; Jiménez-Osés, G.; Houk, K. N.; Garcia-Garibay, M. A. Thermodynamic Evaluation of Aromatic CH/π Interactions and Rotational Entropy in a Molecular Rotor. *J. Am. Chem. Soc.* **2015**, *137*, 2175−2178.

(5) Arcos-Ramos, R.; Rodriguez-Molina, B.; Gonzalez-Rodriguez, E.; Ramirez-Montes, P. I.; Ochoa, M. E.; Santillan, R.; Farfán, N.; Garcia-Garibay, M. A. Crystalline arrays of molecular rotors with TIPS-trityl and phenolic-trityl stators using phenylene, 1,2-difluorophenylene and pyridine rotators. *RSC Adv.* **2015**, *5*, 55201−55208.

(6) Jiang, X.; O'Brien, Z. J.; Yang, S.; Lai, L. H.; Buenaflor, J.; Tan, C.; Khan, S.; Houk, K. N.; Garcia-Garibay, M. A. Crystal Fluidity Reflected by Fast Rotational Motion at the Core, Branches, and Peripheral Aromatic Groups of a Dendrimeric Molecular Rotor. *J. Am. Chem. Soc.* **2016**, *138*, 4650−4656.

(7) Catalano, L.; Perez-Estrada, S.; Wang, H.-H.; Ayitou, A. J.-L.; Khan, S. I.; Terraneo, G.; Metrangolo, P.; Brown, S.; Garcia-Garibay, M. A. Rotational Dynamics of Diazabicyclo[2.2.2]octane in Isomorphous Halogen-Bonded Co-crystals: Entropic and Enthalpic Effects. *J. Am. Chem. Soc.* **2017**, *139*, 843−848.

(8) Setaka, W.; Yamaguchi, K. Order−Disorder Transition of Dipolar Rotor in a Crystalline Molecular Gyrotop and Its Optical Change. *J. Am. Chem. Soc.* **2013**, *135*, 14560−14563 and earlier work cited therein.

(9) Setaka, W.; Inoue, K.; Higa, S.; Yoshigai, S.; Kono, H.; Yamaguchi, K. Synthesis of Crystalline Molecular Gyrotops and Phenylene Rotation inside the Cage. *J. Org. Chem.* **2014**, *79*, 8288−8295.

(10) Setaka, W.; Higa, S.; Yamaguchi, K. Ring-closing metathesis for the synthesis of a molecular gyrotop. *Org. Biomol. Chem.* **2014**, *12*, 3354−3357.

(11) Shionari, H.; Inagaki, Y.; Yamaguchi, K.; Setaka, W. A pyrene-bridged macrocage showing no excimer fluorescence. *Org. Biomol. Chem.* **2015**, *13*, 10511−10516.

(12) Nishiyama, Y.; Inagaki, Y.; Yamaguchi, K.; Setaka, W. 1,4-Naphthalenediyl-Bridged Molecular Gyrotops: Rotation of the Rotor and Fluorescence in Solution. *J. Org. Chem.* **2015**, *80*, 9959−9966.

(13) Masuda, T.; Arase, J.; Inagaki, Y.; Kawahata, M.; Yamaguchi, K.; Ohhara, T.; Nakao, A.; Momma, H.; Kwon, E.; Setaka, W. Molecular Gyrotops with a Five-Membered Heteroaromatic Ring: Synthesis,

DOI: 10.1021/acs.organomet.8b00345
Organometallics 2018, 37, 2991−3000

Temperature-Dependent Orientation of Dipolar Rotors inside the Crystal, and its Birefringence Change. *Cryst. Growth Des.* **2016**, *16*, 4392−4401.
(14) Kottas, G. S.; Clarke, L. I.; Horinek, D.; Michl, J. Artificial Molecular Rotors. *Chem. Rev.* **2005**, *105*, 1281−1376.
(15) Nawara-Hultzsch, A. J.; Skopek, K.; Shima, T.; Barbasiewicz, M.; Hess, G. D.; Skaper, D.; Gladysz, J. A. Syntheses and Palladium, Platinum, and Borane Adducts of Symmetrical Trialkylphosphines with Three Terminal Vinyl Groups, $P((CH_2)mCH{=}CH_2)_3$. *Z. Naturforsch., B: J. Chem. Sci.* **2010**, *65*, 414−424.
(16) Nawara, A. J.; Shima, T.; Hampel, F.; Gladysz, J. A. Gyroscope-like Molecules Consisting of PdX_2/PtX_2 Rotators Encased in Three-Spoke Stators: Synthesis via Alkene Metathesis, and Facile Substitution and Demetalation. *J. Am. Chem. Soc.* **2006**, *128*, 4962−4963.
(17) Nawara-Hultzsch, A. J.; Stollenz, M.; Barbasiewicz, M.; Szafert, S.; Lis, T.; Hampel, F.; Bhuvanesh, N.; Gladysz, J. A. Gyroscope-Like Molecules Consisting of PdX_2/PtX_2 Rotators within Three-Spoke Dibridgehead Diphosphine Stators: Syntheses, Substitution Reactions, Structures, and Dynamic Properties. *Chem. - Eur. J.* **2014**, *20*, 4617−4637.
(18) Shima, T.; Hampel, F.; Gladysz, J. A. Molecular Gyroscopes: $\{Fe(CO)_3\}$ and $\{Fe(CO)_2(NO)\}^+$ Rotators Encased in Three-Spoke Stators; Facile Assembly by Alkene Metatheses. *Angew. Chem., Int. Ed.* **2004**, *43*, 5537−5540; Molekulare Gyroskope: $Fe(CO)_3$- und $Fe(CO)_2(NO)^+$-Rotatoren in einem Stator aus drei Speichen; Einfache Synthese durch Alken-Metathese. *Angew. Chem.* **2004**, *116*, 5653−5656.
(19) Lang, G. M.; Shima, T.; Wang, L.; Cluff, K. J.; Skopek, K.; Hampel, F.; Blümel, J.; Gladysz, J. A. Gyroscope-Like Complexes Based on Dibridgehead Diphosphine Cages That Are Accessed by Three-Fold Intramolecular Ring Closing Metatheses and Encase $Fe(CO)_3$, $Fe(CO)_2(NO)^+$, and $Fe(CO)_3(H)^+$ Rotators. *J. Am. Chem. Soc.* **2016**, *138*, 7649−7663.
(20) Lang, G. M.; Skaper, D.; Hampel, F.; Gladysz, J. A. Synthesis, reactivity, structures, and dynamic properties of gyroscope like iron complexes with dibridgehead diphosphine cages: pre- *vs* post-metathesis substitutions as routes to adducts with neutral dipolar $Fe(CO)(NO)(X)$ rotors. *Dalton Trans.* **2016**, *45*, 16190−16204.
(21) Fiedler, T.; Bhuvanesh, N.; Hampel, F.; Reibenspies, J. H.; Gladysz, J. A. Gyroscope like molecules consisting of trigonal or square planar osmium rotators within three-spoked dibridgehead diphosphine stators: syntheses, substitution reactions, structures, and dynamic properties. *Dalton Trans.* **2016**, *45*, 7131−7147.
(22) Hess, G. D.; Fiedler, T.; Hampel, F.; Gladysz, J. A. Octahedral Gyroscope-like Molecules Consisting of Rhenium Rotators within Cage-like Dibridgehead Diphosphine Stators: Syntheses, Substitution Reactions, Structures, and Dynamic Properties. *Inorg. Chem.* **2017**, *56*, 7454−7469.
(23) Joshi, H.; Kharel, S.; Ehnbom, A.; Skopek, K.; Hess, G. D.; Fiedler, T.; Hampel, F.; Bhuvanesh, N.; Gladysz, J. A. Three Fold Intramolecular Ring Closing Alkene Metatheses of Square Planar Complexes with *cis* Phosphorus Donor Ligands $P(X(CH_2)m\ CH{=}CH_2)_3$ (X/*m*= − /5−10, O/3−5); Syntheses, Structures, and Thermal Properties of Macrocyclic Dibridgehead Diphosphorus Complexes. *J. Am. Chem. Soc.* **2018**, *140*, 8463−8478.
(24) See also: Steigleder, E.; Shima, T.; Lang, G. M.; Ehnbom, A.; Hampel, F.; Gladysz, J. A. Partially Shielded $Fe(CO)_3$ Rotors: Syntheses, Structures, and Dynamic Properties of Complexes with Doubly *trans* Spanning Diphosphines, *trans*-$Fe(CO)_3(PhP((CH_2)_n)_2PPh)$. *Organometallics* **2017**, *36*, 2891−2901.
(25) Stollenz, M.; Taher, D.; Bhuvanesh, N.; Reibenspies, J. H.; Baranová, Z.; Gladysz, J. A. Steric control of the *in*/*out* sense of bridgehead substituents in macrobicyclic compounds: isolation of new "crossed chain" variants of *in*/*out* isomers. *Chem. Commun.* **2015**, *51*, 16053−16056.
(26) Kharel, S.; Jia, T.; Bhuvanesh, N.; Reibenspies, J. H.; Blümel, J.; Gladysz, J. A. A Non-Templated Route to Macrocyclic Dibridgehead Diphosphorus Compounds: Crystallographic Characterization of a "Crossed Chain" Variant of *in*/*out* Stereoisomers. *Chem. - Asian J.* **2018**, DOI: 10.1002/asia.201800739.
(27) Hartley, F. R. Starting Materials for Preparation of Organometallic Complexes of Platinum and Palladium. *Organomet. Chem. Rev. A* **1970**, *6*, 119−137.
(28) Stollenz, M.; Barbasiewicz, M.; Nawara-Hultzsch, A. J.; Fiedler, T.; Laddusaw, R. M.; Bhuvanesh, N.; Gladysz, J. A. Dibridgehead Diphosphines that Turn Themselves Inside Out. *Angew. Chem., Int. Ed.* **2011**, *50*, 6647−6651; Dreifach-verbrückte Diphosphine mit von innen nach außen invertierender Konfiguration. *Angew. Chem.* **2011**, *123*, 6777−6781.
(29) See also: Estrada, A. L.; Jia, T.; Bhuvanesh, N.; Blümel, J.; Gladysz, J. A. Substitution and Catalytic Chemistry of Gyroscope-Like Complexes Derived from Cl−Rh−CO Rotators and Triply *trans* Spanning Di(trialkylphosphine) Ligands. *Eur. J. Inorg. Chem.* **2015**, *2015*, 5318−5321.
(30) Kharel, S.; Joshi, H.; Bierschenk, S.; Stollenz, M.; Taher, D.; Bhuvanesh, N.; Gladysz, J. A. Homeomorphic Isomerization as a Design Element in Container Molecules; Binding, Displacement, and Selective Transport of MCl_2 Species (M = Pt, Pd, Ni). *J. Am. Chem. Soc.* **2017**, *139*, 2172−2175.
(31) Grim, S. O.; Keiter, R. L.; McFarlane, W. A Phosphorus-31 Nuclear Magnetic Resonance Study of Tertiary Phosphine Complexes of Platinum(II). *Inorg. Chem.* **1967**, *6*, 1133−1137.
(32) A reviewer has posed several general questions with respect to Schemes 1, 2, 4, and 5. We have seen no evidence for products with different macrocycle sizes that might be derived via initial C═C isomerizations of the educts. Also, higher educt concentrations have been employed with the metatheses in Scheme 4, but yields decreased. Only in special cases has it proven possible to equilibrate oligomeric and monometallic products (something that must always be carried out prior to hydrogenation).[33] Product distributions are otherwise thought to reflect kinetic control.
(33) Shima, T.; Bauer, E. B.; Hampel, F.; Gladysz, J. A. Alkene metatheses in transition metal coordination spheres: dimacrocyclizations that join *trans* positions of square-planar platinum complexes to give topologically novel diphosphine ligands. *Dalton Trans.* **2004**, *33*, 1012−1028.
(34) Relevant $^{31}P\{^1H\}$ NMR data ($CDCl_3$) for isolated complexes from this work and ref 23 are as follows: *trans*/*cis*-**1f**, 5.1/0.97; *trans*/*cis*-**1g**, 4.7/0.92; *trans*-**1k**, 4.7; *trans*/*cis*-**2f**, 5.1/2.8; *trans*/*cis*-**2g**, 4.9/2.3; *trans*/*cis*-**2k**, 4.7/1.8.
(35) Louw, W. J. Preparative and Kinetic Study on the Mechanisms of Isomerization of Square-Planar Complexes. Kinetic Evidence for Pseudorotation of a Five-Coordinate Intermediate. *Inorg. Chem.* **1977**, *16*, 2147−2160.
(36) Cooper, M. K.; Downes, J. M. Chelate Complexes of Phosphorus−Nitrogen Ligands. 1. Deprotonaton, Cis-Trans Isomerism, and Anion-Catalyzed Isomerization in Platinum(II) Complexes of (*o*-Aminophenyl)diphenylphosphine. *Inorg. Chem.* **1978**, *17*, 880−884.
(37) Anderson, G. K.; Cross, R. J. Isomerization Mechanisms of Square Planar Complexes. *Chem. Soc. Rev.* **1980**, *9*, 185−215.
(38) Rigamonti, L.; Forni, A.; Manassero, M.; Manassero, C.; Pasini, A. Cooperation between Cis and Trans Influences in cis-$Pt^{II}(PPh_3)_2$ Complexes: Structural, Spectroscopic, and Computational Studies. *Inorg. Chem.* **2010**, *49*, 123−135 and earlier work cited therein.
(39) For analogous bond length trends in a complex with both *cis*- and *trans*-$PtCl_2(PArMe_2)_2$ units, see Table 1 of Drahoš, B.; Rohlik, Z.; Kotek, J.; Císařová, I.; Hermann, P. Complexes of hydrophilic triphenylphosphines modified with *gem*-bis(phosphonate) moiety. An unusual simultaneous *cis* and *trans* arrangements in the Pt(II) dinuclear complex. *Dalton Trans.* **2009**, *48*, 4942−4953.
(40) Balachander, N.; Sukenik, C. N. Monolayer Transformation by Nucleophilic Substitution: Applications to the Creation of New Monolayer Assemblies. *Langmuir* **1990**, *6*, 1621−1627.
(41) Effenberger, F.; Heid, S. Synthesis of Model Compounds for the Formation of Self-Assembled Monolayers on a Silicon Surface. *Synthesis* **1995**, 1126−1130.

DOI: 10.1021/acs.organomet.8b00345
Organometallics 2018, 37, 2991−3000

(42) Sanford, M. S.; Love, J. A.; Grubbs, R. H. Mechanism and Activity of Ruthenium Olefin Metathesis Catalysts. *J. Am. Chem. Soc.* **2001**, *123*, 6543−6554.
(43) Fürstner, A.; Thiel, O. R.; Ackermann, L.; Schanz, H.-J.; Nolan, S. P. Ruthenium Carbene Complexes with *N,N′*-Bis(mesityl)imidazol-2-ylidene Ligands: RCM Catalysts of Extended Scope. *J. Org. Chem.* **2000**, *65*, 2204−2207.
(44) Evans, P.; Grigg, R.; Monteith, M. Metathesis of aniline and 1,2-dihydroquinoline derivatives. *Tetrahedron Lett.* **1999**, *40*, 5247−5250.
(45) Marvey, B. B.; Segakweng, C. K.; Vosloo, M. H. C. Ruthenium Carbene Mediated Metathesis of Oleate-Type Fatty Compounds. *Int. J. Mol. Sci.* **2008**, *9*, 615−625.
(46) Martinez, A.; Gutiérrez, S.; Tlenkopatchev, M. A. Citrus oils as chain transfer agents in the cross-metathesis degradaton of polybutadiene in block copolymers using Ru-alkylidene catalysts. *Nat. Sci.* **2013**, *5*, 857−864.
(47) Roux, M.-C.; Paugam, R.; Rousseau, G. Evaluation of *exo-endo* Ratios in the Halolactonization of Ω-Unsaturated Acids. *J. Org. Chem.* **2001**, *66*, 4304−4310.
(48) The P$CH_2CH_2CH_2$ ^{1}H and ^{13}C NMR signal assignments of the free phosphines were confirmed by ^{1}H,^{1}H COSY and ^{1}H,^{13}C{^{1}H} COSY experiments. The corresponding signals in the platinum complexes were assigned by analogy to those of closely related complexes reported earlier.[17] Representative 2D NMR spectra that provide the basis for these assignments have been published.[21,49]
(49) Lang, G. M.; Skaper, D.; Shima, T.; Otto, M.; Wang, L.; Gladysz, J. A. Syntheses of Iron(0) Complexes of Symmetrical Trialkylphosphines with Three Terminal Vinyl Groups, P((CH2)*m* CH═CH2)3. *Aust. J. Chem.* **2015**, *68*, 1342−1351.
(50) The *J* values given for virtual triplets represent the *apparent* couplings between adjacent peaks and not the mathematically rigorous coupling constants. See: Hersh, W. H. False AA'X Spin-Spin Coupling Systems in ^{13}C NMR: Examples Involving Phosphorus and a 20-Year-Old Mystery in Off-Resonance Decoupling. *J. Chem. Educ.* **1997**, *74*, 1485−1488.
(51) This coupling represents a satellite (d, ^{195}Pt = 33.8%) and is not reflected in the peak multiplicity given.
(52) *APEX3*; Bruker AXS Inc.: Madison, WI, 2012.
(53) Sheldrick, G. M. *SADABS*; Bruker AXS Inc.: Madison, WI, 2001.
(54) Sheldrick, G. M. A short history of *SHELX*. *Acta Crystallogr., Sect. A: Found. Crystallogr.* **2008**, *64*, 112−122.
(55) Sheldrick, G. M. SHELXT − Integrated space-group and crystal structure determination. *Acta Crystallogr., Sect. A: Found. Adv.* **2015**, *71*, 3−8.
(56) Sheldrick, G. M. Crystal structure refinement with *SHELXL*. *Acta Crystallogr., Sect. C: Struct. Chem.* **2015**, *71*, 3−8.
(57) Dolomanov, O. V.; Bourhis, L. J.; Gildea, R. J.; Howard, J. A. K.; Puschmann, H. OLEX2: A Complete Structure Solution, Refinement and Analysis Program. *J. Appl. Crystallogr.* **2009**, *42*, 339−341.
(58) Spek, A. L. Single-crystal structure validation with the program *PLATON*. *J. Appl. Crystallogr.* **2003**, *36*, 7−13.

DOI: 10.1021/acs.organomet.8b00345
Organometallics 2018, 37, 2991−3000